© 2015. Published by The Company of Biologists Ltd | Journal of Experimental Biology (2015) 218, 3032-3041 doi:10.1242/jeb.125310

RESEARCH ARTICLE

Lipid composition and molecular interactions change with depth in the avian stratum corneum to regulate cutaneous water loss

Alex M. Champagne[1,*], Heather C. Allen[2,3] and Joseph B. Williams[4]

ABSTRACT

The outermost 10–20 µm of the epidermis, the stratum corneum (SC), consists of flat, dead cells embedded in a matrix of intercellular lipids. These lipids regulate cutaneous water loss (CWL), which accounts for over half of total water loss in birds. However, the mechanisms by which lipids are able to regulate CWL and how these mechanisms change with depth in the SC are poorly understood. We used attenuated total reflectance Fourier transform infrared spectroscopy (ATR-FTIR) to measure lipid–lipid and lipid–water interactions as a function of depth in the SC of house sparrows (*Passer domesticus* Linnaeus) in the winter and summer. We then compared these molecular interactions at each depth with lipid composition at the same depth. We found that in both groups, water content increased with depth in the SC, and likely contributed to greater numbers of gauche defects in lipids in deeper levels of the SC. In winter-caught birds, which had lower rates of CWL than summer-caught birds, water exhibited stronger hydrogen bonding in deeper layers of the SC, and these strong hydrogen bonds were associated with greater amounts of polar lipids such as ceramides and cerebrosides. Based on these data, we propose a model by which polar lipids in deep levels of the SC form strong hydrogen bonds with water molecules to increase the viscosity of water and slow the permeation of water through the SC.

KEY WORDS: Lipids, Skin, Infrared spectroscopy, Birds, Tape stripping

INTRODUCTION

In birds, total evaporative water loss has been shown to be the major route of water loss, accounting for five times the water lost through urine and feces in many small species (Williams and Tieleman, 2005, 2000; Bartholomew, 1972; Dawson, 1982). Because cutaneous water loss (CWL) accounts for approximately 65% of total evaporative water loss (Tieleman and Williams, 2002; Ro and Williams, 2010), the rate of CWL plays an important role in determining water and heat balance in birds (Champagne et al., 2012; Muñoz-Garcia and Williams, 2007). The primary barrier to CWL, the stratum corneum (SC) spans the outermost 10–20 µm of the avian integument, and is composed of flat, dead cells called corneocytes connected by protein bridges called corneodesmosomes, all embedded within a lipid matrix (Bouwstra, 1997). Some lipids within the matrix of the SC are covalently bound to the corneocytes (Wertz and Downing, 1987; Gu et al., 2008), whereas others occupy the intercellular space in layers called lamellae (Wertz and Downing, 1982). These lamellar lipids are arranged in either bilayers (Wertz and Downing, 1982; Champagne et al., 2012) or trilayers (Bouwstra et al., 2000; Muñoz-Garcia et al., 2008a), and appear to serve as the primary barrier to CWL (Clement et al., 2012). Lamellar lipids in the avian SC consist primarily of cholesterol esters, fatty acid methyl esters, triacylglycerols, free fatty acids, cholesterol, ceramides and cerebrosides, the last of these being a ceramide with a glucose moiety attached to the headgroup (Menon et al., 1986; Haugen et al., 2003; Muñoz-Garcia et al., 2006; Ro and Williams, 2010). The composition and attendant organization of these lipid classes affects the rate of CWL (Champagne et al., 2012). Previous studies on birds have found that higher amounts of free fatty acids and triacylglycerols within the SC are associated with higher rates of CWL, whereas more polar ceramides and cerebrosides are associated with lower rates of CWL (Haugen et al., 2003; Muñoz-Garcia et al., 2008a,b; Champagne et al., 2012). Cerebrosides are thought to be especially important in regulating CWL, as they account for approximately one-third of all lipids in the SC in birds, and occur in greater amounts in the SC of birds acclimated to cold, dry conditions than in birds acclimated to warmer, more humid conditions (Muñoz-Garcia et al., 2008a). The potential role of cerebrosides in reducing water loss in birds is especially striking because cerebrosides are not present in mammalian skin except in individuals with a pathological condition called Gaucher disease, a disease characterized by dry, scaly skin and abnormally high rates of CWL. In humans with Gaucher disease, CWL is thought to be higher because the bulky sugar moieties of cerebrosides disrupt packing of the lamellar lipids (Holleran et al., 1994). The observation that cerebrosides exert an opposite effect on CWL to that seen in mammals suggests that the mechanisms by which lipids of the SC interact with each other and with water remain a fundamental problem that we do not understand in birds, or in humans with Gaucher disease.

Although it is generally agreed that water passes through lipid lamellae as it diffuses through the SC (Simonetti et al., 1995; Meuwissen et al., 1998), the specific molecular interactions that occur between lipid and water molecules during the diffusional process are relatively unknown. It is thought that water molecules permeate through lamellae by inserting between hydrophilic lipid headgroups to increase spacing between lipid molecules (Golden et al., 1986; Alonso et al., 1996). This increase in intermolecular distance disrupts the normal *trans* configuration of the hydrophobic alkyl chains of the lipids and causes some carbon–carbon bonds to rotate approximately 120 deg to create gauche defects in the alkyl chains. Because of these defects, 'kinks' appear in the alkyl chains, with more severe kinks appearing when the gauche defect occurs close to the lipid headgroup rather than near the ω end of the chain (Liang et al., 1994). The kinks caused by the gauche defects create 'holes' in the hydrophobic space of the lamellae through which

[1]Department of Biology, University of Southern Indiana, Science Center 1255 8600 University Blvd, Evansville, IN 47712, USA. [2]Department of Chemistry and Biochemistry, The Ohio State University, 1102 Newman and Wolfrom Laboratory, 100 W 18th Avenue, Columbus, OH 43210, USA. [3]Department of Pathology, The Ohio State University, 129 Hamilton Hall, 1645 Neil Avenue, Columbus, OH 43210, USA. [4]Department of Evolution, Ecology, and Organismal Biology, The Ohio State University, Aronoff Laboratory, 318 W 12th Avenue, Columbus, OH 43210, USA.

*Author for correspondence (achampagne@usi.edu)

Received 14 May 2015; Accepted 27 July 2015

Journal of Experimental Biology

Journal of Experimental Biology (2015) 218, 3032-3041 doi:10.1242/jeb.125310

water molecules can pass and thus the number of gauche defects may indicate the rate at which water is moving through the SC (Potts and Francoeur, 1990).

In addition to the intermolecular interactions taking place in the hydrophobic space within lamellae, hydrophilic interactions between water and lipid headgroups may also influence CWL. In birds, ceramide and cerebroside headgroups are thought to play a major role in preventing water permeation through lipid layers, as more polar headgroups may form strong hydrogen bonds with each other and consequently influence water infiltration (Adams and Allen, 2013). In current models of lipid organization within the avian SC, glucose moieties of cerebrosides project into the hydrophilic space outside lipid layers (Champagne et al., 2012). Because of this orientation, the sugar moieties of cerebrosides may slow the rate of CWL by forming strong hydrogen bonds with adjacent water molecules to form a primary solvation shell (Bach et al., 1982). Although these strong hydrogen bonds weaken the hydrogen bonding of water molecules outside the solvation shell (Gallina et al., 2006), the strong hydrogen bonds formed within the solvation shell increase the overall viscosity of the water, which may slow the rate of permeation through the SC (Comesaña et al., 2003; Clement et al., 2012; Champagne et al., 2012). Current models remain speculative and do not address variation in molecular interactions in different layers of the SC, or how this variation affects the rate of CWL.

Although most studies correlating barrier properties of the SC with lipid composition have assumed uniform water flux and lipid composition throughout the thickness of the SC, several studies on human SC have shown that water content increases in deeper layers of the SC (Warner et al., 1988; Bommannan et al., 1990; Boncheva et al., 2009). Furthermore, tape-stripping experiments on human SC show that overall lipid content decreases with depth in the uppermost 2 µm of the SC as corneocyte volume increases, and remains constant thereafter (Bommannan et al., 1990). The composition of lamellar lipids in human SC also changes with depth, as the proportion of free fatty acids decreases by over half whereas ceramides and cholesterol exhibit small proportional increases with depth (Bonté et al., 1997; Weerheim and Ponec, 2001). The high proportion of free fatty acids in the upper 2 µm of human SC is thought to cause the greater amount of gauche defects observed by infrared spectroscopy in this layer (Bommannan et al., 1990).

Human models of lipid content and molecular organization throughout the depth of the SC are inappropriate for predicting the depth profile of avian SC and assessing its effects on CWL for several reasons. First, some of the free fatty acids in the upper SC of humans are sebaceous in origin (Bommannan et al., 1990), and birds lack sebaceous glands (Matoltsy, 1969). Second, healthy human SC does not contain cerebrosides, which may affect water content and the strength of hydrogen bonding among lipid and water molecules in avian SC. Finally, the effects of acclimation to different temperature and humidity regimes on the depth profile of the SC have not been investigated, despite the fact that these variables affect CWL in birds (Muñoz-Garcia et al., 2008a).

In this study, we integrated methods in physical chemistry, analytical chemistry and whole-organism physiology to understand how the SC of birds regulates CWL in response to changes in their environment. We first used tape stripping and attenuated total reflectance Fourier transform infrared spectroscopy (ATR-FTIR) to assess hydrogen bond strength, the relative amount of gauche defects in lipid alkyl chains, and water content throughout 10 layers of the SC in house sparrows (*Passer domesticus* Linnaeus) acclimatized to either a cold, dry winter environment or a warm, humid summer environment. We correlated information on these molecular interactions with the lipid composition of each layer and related both data sets with changes in CWL that we observed between seasons. Our results offer compelling evidence that the distribution of water and lipids is not uniform with depth in avian SC, and these differences in water and lipid content correlate with concurrent changes in water–water and water–lipid interactions. Water and lipid content and their associated molecular interactions also change seasonally, which is reflected in changes in CWL, and these changes may help birds maintain heat and water balance in disparate environmental conditions.

RESULTS

CWL

House sparrows captured in the summer lost an average of 47.78 mg H_2O cm^{-2} per day through their skin, whereas birds captured in the winter averaged 25.87 mg H_2O cm^{-2} per day, a difference that was significant (t_{16}=4.12, P=0.001).

Depth of the SC

The depth of SC removed from the surface of each house sparrow via tape stripping varied as a function of tape strip number ($F_{1,15.3}$=1057.74, P<0.001), season ($F_{1,129.2}$=38.62, P<0.001), and the interaction ($F_{1,137.7}$=61.35, P<0.001). Tape strips of house sparrows captured in the summer removed 0.43±0.04 µm of SC with the first tape strip and 0.23±0.01 µm SC with subsequent strips. Tape strips of house sparrows captured in the winter removed 0.19±0.03 µm with the first strip and 0.16±0.01 µm per strip thereafter (Fig. 1; $F_{3,140}$=1132.81, P<0.001, R^2=0.96). The amount of SC removed from winter- and summer-caught birds differed significantly for the first strip (P<0.001) and for the rate of removal (P<0.001).

ATR spectra

We identified five peaks of absorbance in our analysis of house sparrow skin: OH stretching peaks at ~3500 and ~3300 cm^{-1}, a CH stretching peak at ~3080 cm^{-1}, a CH_2 asymmetric stretching peak at ~2950 cm^{-1}, a CH_2 symmetric stretching peak at ~2850 cm^{-1}, and an H_2O combination band at ~2100 cm^{-1} (Fig. 2). The first OH stretching peak (~3500 cm^{-1}) had a mean absorbance peak of 3458.06±7.34 cm^{-1} at the skin surface and increased linearly at a rate of 17.80±3.52 cm^{-1} $µm^{-1}$ SC exposed by tape stripping in both groups of birds (supplementary material Fig. S1A; $F_{1,139.37}$=25.62, P<0.001). The second OH stretching peak (~3300 cm^{-1}) absorbed

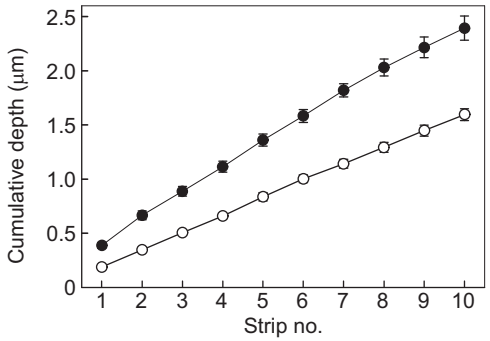

Fig. 1. Increase in stratum corneum (SC) depth as a function of tape strip number for summer and winter house sparrows. Summer birds are indicated by black circles, and winter birds by white circles. Error bars indicate standard error for each tape strip.

Journal of Experimental Biology (2015) 218, 3032-3041 doi:10.1242/jeb.125310

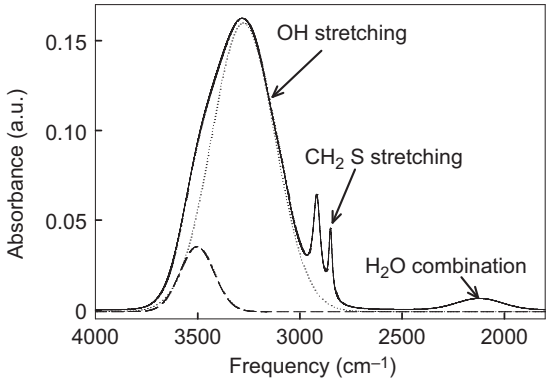

Fig. 2. Absorbance spectrum from a layer of house sparrow SC for wavenumbers between 4000 and 1800 cm^{-1}. OH stretching, CH_2 symmetric (S) stretching and H_2O combination absorbance regions are indicated by arrows. The OH stretching region is shown with two component peaks separated by peak-fitting software into a peak at ~3500 cm^{-1} (dashed line) and a peak at ~3300 cm^{-1} (dotted line).

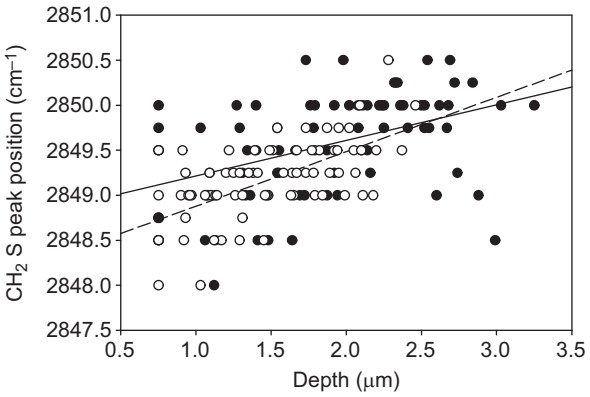

Fig. 4. Change in the peak position for the CH_2 symmetric stretching peak as a function of depth for both treatment groups. Summer birds are indicated by black circles and a solid line, winter birds are indicated by white circles and a dashed line. Depth is based on the maximum penetration of an evanescent wave at 2850 cm^{-1}.

light at a mean of 3263.64±4.84 cm^{-1} at the skin surface of winter birds and 3250.72±5.34 cm^{-1} in summer birds ($F_{1,16.68}$=5.85, P=0.027). The peak increased linearly in frequency in both groups of birds at a rate of 8.70±2.07 cm^{-1} μm^{-1} (supplementary material Fig. S1B; $F_{1,137.84}$=17.62). These data may indicate a slight decrease in intermolecular hydrogen bond strength in deeper layers, although these peak positions may be interfered with by other nearby peaks (Miranda et al., 1998; Wolkers et al., 2004; Tang et al., 2011). However, with increasing SC depth, the ratio of the area of the ~3300 cm^{-1} OH stretching peak relative to the area of the ~3500 cm^{-1} peak increased in both groups of birds ($F_{1,137.42}$=14.72, P<0.001) indicating an increase in the number of strong intermolecular hydrogen bonds or overall hydrogen bonding strength as a function of depth. This ratio also differed between seasons ($F_{1,108.97}$=5.64, P=0.02) and with the interaction between depth and season ($F_{1,137.42}$=11.41, P=0.001). Overall, the ratio increased at a higher rate in winter birds, though summer birds exhibited a higher initial ratio (Fig. 3). These data indicate stronger intermolecular hydrogen bonding in deeper layers of the SC in winter birds than in summer birds.

The CH_2 symmetric stretching peak absorbed IR light at a frequency of 2848.42±0.12 cm^{-1} at the skin surface and frequency increased linearly with depth at a rate of 0.50±0.06 cm^{-1} μm^{-1} SC exposed by tape stripping in both groups of birds (Fig. 4; $F_{1,145.57}$=64.56, P<0.001), indicating an increase in gauche defects as a function of depth.

The area of the H_2O combination band increased as a function of depth ($F_{1,138.35}$=152.68, P<0.001) and increased at a greater rate in summer birds (Fig. 5; $F_{1,138.35}$=4.62, P=0.03), indicating increasing water content in deeper layers of the SC, especially in summer birds. Additionally, this increasing water content was positively correlated with the relative amount of gauche conformers in lipids ($F_{1,150}$=196.08, P<0.001, R^2=0.57). However, the amount of water did not affect the strength of intermolecular hydrogen bonding as measured by the ratio of the ~3300 cm^{-1} to the ~3500 cm^{-1} peaks ($F_{1,150}$=0.236, P=0.63).

Lipids

In each layer of the SC, we identified cholesterol ester, fatty acid methyl ester, triacylglycerols, free fatty acid, cholesterol, ceramide I, ceramide II and cerebroside (supplementary material Fig. S2). As SC depth increased, total lipid content relative to protein increased in both groups of birds ($F_{1,123.08}$=4.13, P=0.04). However, winter birds had greater total lipid content in superficial layers of the SC, and thus had

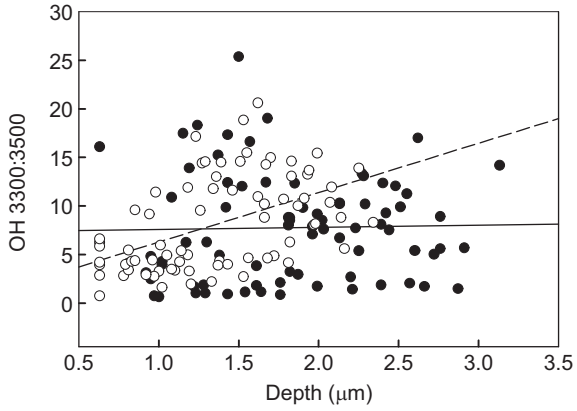

Fig. 3. Change in the ratio of the low energy OH stretching peak (~3300 cm^{-1}) to the high energy OH stretching peak (~3500 cm^{-1}). Summer birds are indicated by black circles and a solid line, winter birds are indicated by white circles and a dashed line. Depth is based on the maximum penetration of an evanescent wave at 3400 cm^{-1}.

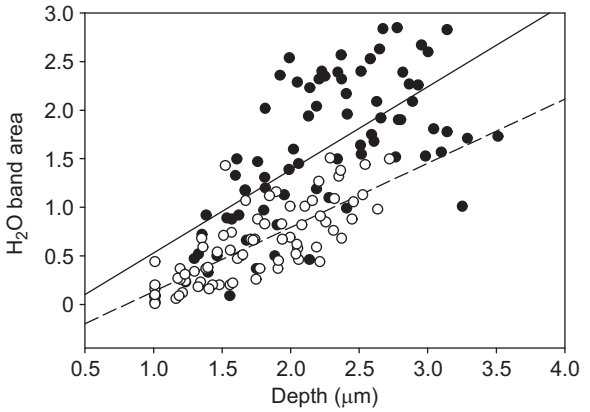

Fig. 5. Change in the H_2O combination band area as a function of depth. Summer birds are indicated by black circles and a solid line, winter birds are indicated by white circles and a dashed line. Depth is based on the maximum penetration of an evanescent wave at 2100 cm^{-1}.

Journal of Experimental Biology (2015) 218, 3032-3041 doi:10.1242/jeb.125310

more lipids overall (Fig. 6A; $F_{1,14.41}$=12.21, P=0.003). All lipid classes showed a linear relationship with SC depth except for cholesterol ester, which varied as an inverse function with depth. Free fatty acids and ceramide I also increased with depth in both groups of birds ($F_{1,17.22}$=6.42, P=0.02 and $F_{1,15.47}$=11.54, P=0.004, respectively), but winter birds had greater amounts of both lipid classes overall (Fig. 6B,C; $F_{1,14.31}$=17.17, P=0.001 and $F_{1,16.25}$=5.62, P=0.03, respectively). Cholesterol ester decreased with depth in both groups of birds ($F_{1,141.68}$=70.14, P<0.001), but this decrease occurred at a higher rate in summer birds (Fig. 7; $F_{1,141.68}$=4.50, P=0.04). Cerebrosides and ceramide II increased with depth in both groups of birds ($F_{1,144.29}$=44.83, P<0.001 and $F_{1,144.31}$=23.66, P<0.001, respectively), but increased at a higher rate in winter birds (Fig. 8A,B; $F_{1,144.29}$=5.23, P=0.02 and $F_{1,144.31}$=7.20, P=0.01, respectively). Cholesterol, triacylglycerols and fatty acid methyl ester content did not change as a function of depth or season.

DISCUSSION

We have shown that water, lipid content and molecular organization change with depth in the SC of birds. Furthermore, we have shown that birds modify the locations of certain lipid classes seasonally, likely to acclimatize to changes in temperature and humidity and thus maintain heat and water balance even in cold, dry conditions.

In both winter- and summer-acclimatized house sparrows, the amount of water increased linearly with SC depth, a pattern that is consistent with studies done on humans (Warner et al., 1988; Boncheva et al., 2009). This increase in water content was positively correlated with the number of gauche defects present in the associated lipid lamellae. These data indicate that more water molecules are permeating through lipid lamellae in the deeper stratum corneum, creating 'holes' in the hydrophobic space of lipid bilayers (Golden et al., 1986; Potts and Francoeur, 1990). In more superficial layers of the SC, fewer gauche defects were observed in lipid chains, which may be related to the lower water content in these

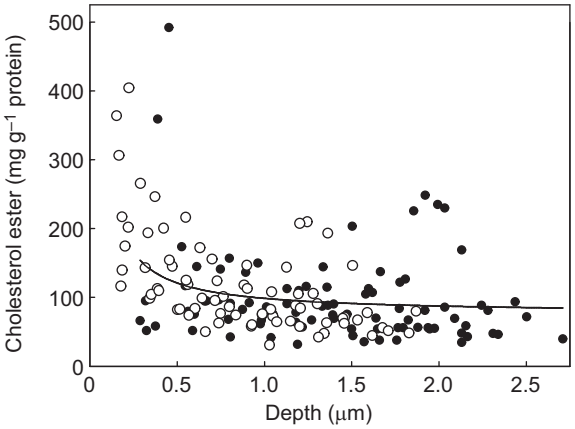

Fig. 7. Change in cholesterol ester concentration for both treatment groups as a function of depth. Summer birds are indicated by black circles and a solid line, winter birds are indicated by white circles and a dashed line.

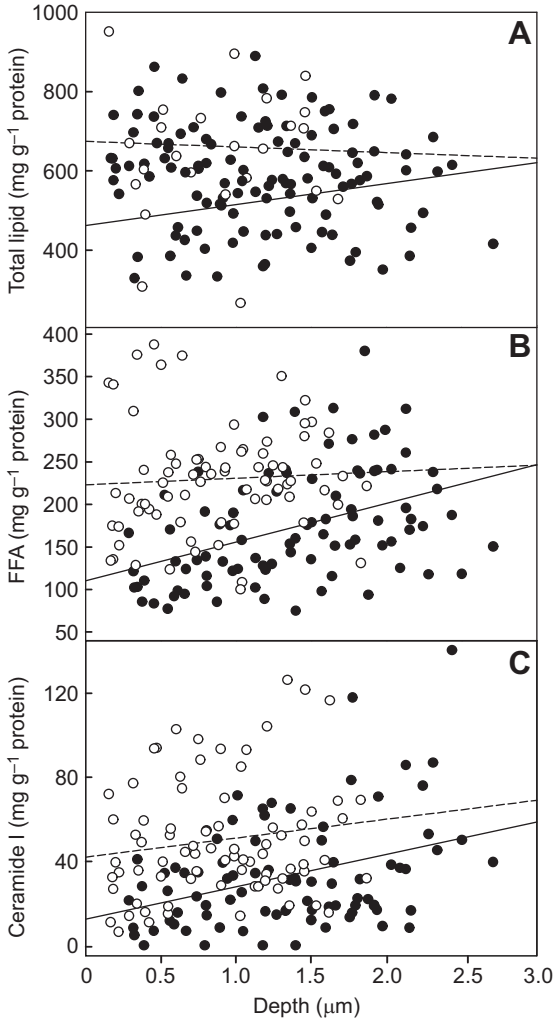

Fig. 6. Change in lipid concentration as a function of depth. (A) Total lipid, (B) free fatty acid (FFA) and (C) ceramide I. Summer birds are indicated by black circles and a solid line, winter birds are indicated by white circles and a dashed line.

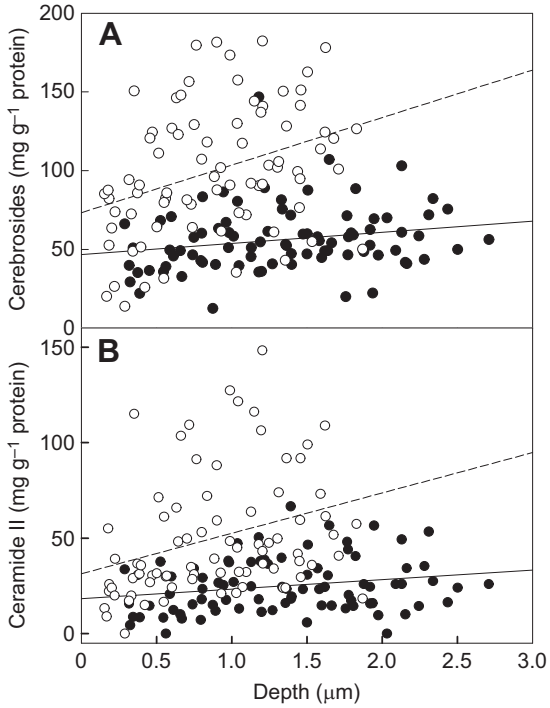

Fig. 8. Change in cerebroside and ceramide II concentration as a function of depth. (A) Cerebroside, (B) ceramide II. Summer birds are indicated by black circles and solid line, winter birds are indicated by white circles and dashed line.

Journal of Experimental Biology (2015) 218, 3032-3041 doi:10.1242/jeb.125310

layers. A second explanation for the smaller number of gauche defects in superficial layers of the SC is that lipid lamellae in these layers often tear apart from one another during the desquamation process (Chapman and Walsh, 1990; Rawlings et al., 1995), thus creating gaps through which water can evaporate without having to pass through lipid bilayers. This non-lipid-mediated evaporative pathway would speed the rate of evaporation in these layers and further reduce the amount of water disrupting lipid bilayers.

In addition to water, lipid composition may also affect the relative number of gauche defects in a lipid bilayer. In general, more polar lipids with short, saturated alkyl chains of uniform length pack more closely, and are thus less prone to gauche defects than lipids that are more non-polar and have long, unsaturated chains of variable length (Casal and McElhaney, 1990; Adams and Allen, 2013). However, we could not find a clear pattern of polarity or chain length with respect to depth in the SC, and our method of thin layer chromatography cannot detect the degree of saturation. These data for house sparrows suggest that unlike in human systems, where the number of gauche defects is negatively associated with water content, but positively associated with free fatty acid content (Bommannan et al., 1990; Bonté et al., 1997; Weerheim and Ponec, 2001), water is the main driver of SC lipid disorder in avian systems.

Despite the fact that gauche defects appeared to be more correlated with water content than with lipid composition, our data suggest that, like in humans, birds exhibit biological control of lipid content throughout the depth of the SC. For example, our finding that cholesterol ester dramatically increases at the surface of the skin in both groups of birds is similar to a pattern found in humans (Freinkel and Aso, 1969). This increase is likely mediated by an acyl-CoA-cholesterol transferase enzyme (Freinkel and Aso, 1971) that is utilized by microbial communities on the surface of the skin (Puhvel, 1975). In addition, cerebrosides, which increased with depth in winter and summer birds, are broken down by β-glucocerebrosidase within the SC (Cox et al., 2008). The action of the enzymes that help modify cholesterol ester, cerebrosides and other lipids is likely affected by the change in pH from neutral in deeper layers to more acidic pH at the surface. In humans, the SC changes from pH 7.0 at the base to pH 5.3–5.8 (Freinkel and Aso, 1969), and β-glucocerebrosidase functions best at pH values ranging from 4.8 to 5.8 (Cox et al., 2008). The patterns we found in cholesterol ester and cerebroside content throughout the thickness of the SC suggest that these enzymes function primarily in superficial layers of the SC, and thus a pH gradient similar to that in humans exists in the SC of birds.

The differences we found in lipid depth profile between winter and summer birds provide evidence that the modifications in lipid composition throughout the depth of the SC affect CWL and are in part a response to changes in environmental temperature and humidity. Winter house sparrows, which were exposed to a low temperature and vapor pressure, lost water at a lower rate than house sparrows caught in the summer. These winter birds had more total SC lipids relative to protein and, strikingly, more polar lipids in deeper levels of the SC. Ceramide II, the more polar group of ceramides, and cerebrosides increased at a greater rate with depth in winter birds than in summer birds, indicating that these lipids play an instrumental role in reducing CWL, especially in the deeper levels of the SC. More polar lipids have been correlated with lower rates of CWL in birds (Haugen et al., 2003; Muñoz-Garcia et al., 2008a,b; Champagne et al., 2012).

The mechanism by which more polar ceramides and cerebrosides inhibit water loss may involve the formation of strong hydrogen bonds between polar lipid headgroups and adjacent lipid headgroups to create a tight packing arrangement (Adams and Allen, 2013).

Additionally, the headgroups of polar lipids may form strong hydrogen bonds with water to alter its structure, thus sequestering it in the SC (Champagne et al., 2012). Changes in the area of the OH stretching peak with depth in our ATR-FTIR data provide evidence that both of these mechanisms may be occurring in the deeper levels of the SC of birds to reduce CWL. As depth increased, the ratio of the ∼3300 cm^{-1} peak area relative to the ∼3500 cm^{-1} peak area increased in both groups of birds, and this increase was greater in winter birds. In general, these changes in the ratio may be attributed to an increase in strong hydrogen bonding among water and hydroxyl groups in deeper levels of the SC (Gallina et al., 2006). The coincidence with depth between stronger hydrogen bonds and more polar lipids such as ceramides and cerebrosides suggests that these polar lipids are forming strong hydrogen bonds with adjacent lipids and with adjacent water molecules as mechanisms of reducing CWL. Although the increase in frequency we observed in both OH stretching peaks as a function of depth indicates weakening of hydrogen bonds and seems to provide contradictory evidence for these mechanisms, these increases in frequency may reflect a decrease in the hydrogen bonding strength of bulk water within the SC, rather than hydrogen bonding between adjacent lipid headgroups or between water and lipid headgroups. Indeed, the hydrogen bonding of the bulk water is weakened as water molecules are attracted by solutes and thus drawn out of a tetrahedral hydrogen bonding structure (Gallina et al., 2006; Paolantoni et al., 2007). Additionally, the frequencies of both OH peaks may have been influenced by increases with depth in the absorbance of glucose from cerebrosides (∼3350 cm^{-1}; Wolkers et al., 2004) or water interacting with carboxylic acid moieties of free fatty acids (∼3600 cm^{-1}; Miranda et al., 1998; Tang et al., 2011).

Forming strong hydrogen bonds with adjacent lipid headgroups within a bilayer is one mechanism by which polar lipids such as ceramides and cerebrosides may reduce CWL. As a result of these strong headgroup interactions, water molecules may be impeded from inserting themselves into spaces between lipid headgroups (Adams and Allen, 2013; Golden et al., 1986; Alonso et al., 1996), thus improving each bilayer's resistance to water permeation. Additionally, headgroup interactions may increase the cohesiveness of the SC in general to make it less susceptible to mechanical stress and therefore better able to maintain intact lipid barriers to water loss (Chapman et al., 1991). The increased cohesiveness we observed in winter-caught house sparrows may be at least partially explained by the fact that these birds had greater amounts of ceramide II and cerebrosides, although corneodesmosome strength between corneocytes typically is more responsible for SC cohesiveness, especially in low humidity environments (Chapman et al., 1991; Simon et al., 2001).

A second mechanism by which polar lipids may reduce CWL is by forming strong hydrogen bonds with adjacent water molecules. The glucose moieties of cerebrosides may be especially important in governing the structure of water, as they are thought to project outside the lipid bilayers (Champagne et al., 2012; Adams and Allen, 2013), where they may interact with four to nine water molecules (Bach et al., 1982). We propose a model by which the glucose moieties of cerebrosides form strong hydrogen bonds with adjacent water molecules to form a primary solvation shell (Fig. 9). As a result, the hydrogen bonds between water molecules in the primary solvation shell and water molecules outside the shell are disrupted, thus weakening hydrogen bonding structure of the water just beyond the solvation shell (Gallina et al., 2006; Paolantoni

Journal of Experimental Biology (2015) 218, 3032-3041 doi:10.1242/jeb.125310

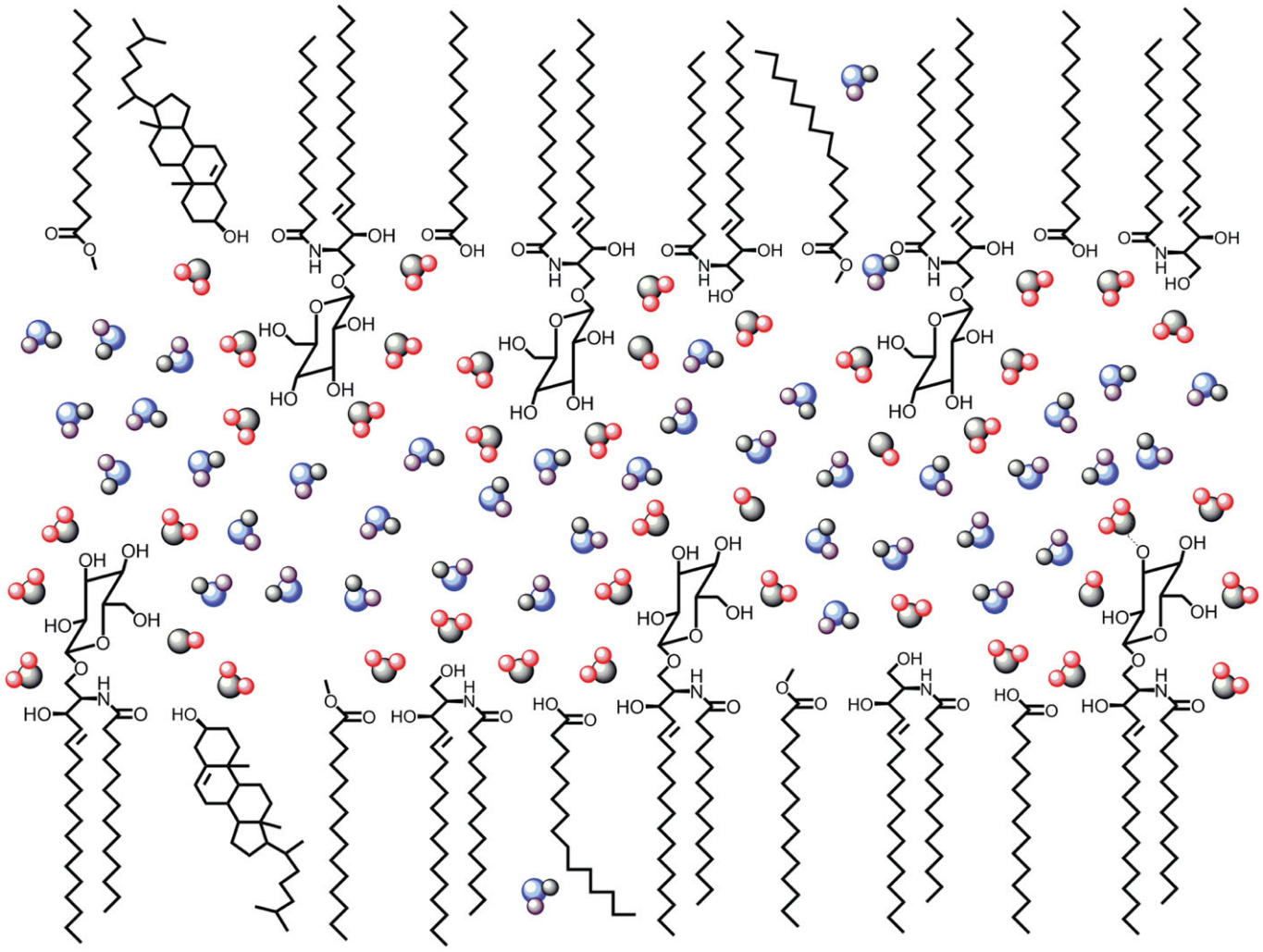

Fig. 9. Model of water organization between lamellar bilayers in the SC. Water molecules and free hydroxyls adjacent to hydroxyl groups on lipid headgroups and glucose moieties of cerebrosides form strong hydrogen bonds with these hydroxyl groups (red and black water molecules and free hydroxyls), whereas the bulk water (black and blue water molecules) forms weaker, but more frequent hydrogen bonds, thus making water more viscous. Water molecules that have broken free of the bulk water will move through the hydrophobic space in lipid bilayers, causing gauche defects to occur in lipid alkyl chains.

et al., 2007). However, despite the weakening of hydrogen bonds in water outside the solvation shell, the strong hydrogen bonding between glucose moieties of cerebrosides and water molecules in the first solvation shell increases the viscosity of the water and potentially slows the rate of water permeation through the SC (Fuchs and Kaatze, 2001; Comesaña et al., 2003).

Another factor that our model takes into consideration is the potential steric hindrance that limits cerebroside molecules from packing too closely together (Maggio et al., 2006; Adams and Allen, 2013). Evidence suggests that when cerebrosides and free fatty acids are mixed, the two form a miscible layer with free fatty acids filling in the gaps between cerebroside molecules (Adams and Allen, 2013). As free fatty acid content increases with SC depth, and thus cerebroside content, we think that these molecules perform a similar function in the deeper layers of the avian SC. Additionally, in deeper layers of the SC where pH may be higher, free fatty acid headgroups may be ionized to create a charged field in the surrounding water molecules, thus further strengthening hydrogen bonding in these layers (Miranda et al., 1998).

In conclusion, we found that water content increases with depth in house sparrow SC. This increase in water content is correlated with the presence of gauche defects in lipid alkyl chains, indicating that water is moving through lipid bilayers in deeper levels of the SC more than in superficial levels, where it may also evaporate through physical gaps in the SC (Chapman and Walsh, 1990; Rawlings et al., 1995). These differences in water content and alkyl chain conformation are associated with changes in lipid content throughout the depth of the SC, and these changes are likely mediated by enzymes (Freinkel and Aso, 1971; Cox et al., 2008). A consistent pattern that we found in lipid composition as a function of depth was that ceramide II and cerebrosides increased with depth, and these increases were more pronounced in winter-caught house sparrows, which had lower rates of CWL. Because these increases in ceramide II and cerebroside coincided with increases in strong hydrogen bonding among water and hydroxyl groups, we hypothesize that birds acclimatized to cold, dry conditions upregulate the production of these lipids in the deeper SC as a mechanism to increase lipid and water cohesion and thus reduce CWL. Previous studies on how glucose affects the structure of water (Gallina et al., 2006; Paolantoni et al., 2007) led us to propose a model by which the glucose moieties of cerebrosides may interact with water molecules to slow the rate of CWL in deeper levels of the SC. Although this model is based on correlative data, further tests with FTIR using deuterated water could separate interactions

Journal of Experimental Biology (2015) 218, 3032-3041 doi:10.1242/jeb.125310

between hydroxyl groups of lipids and interactions between water molecules. These tests will allow us to better understand the mechanism by which cerebrosides and other lipids interact with water to alter its structure and produce a barrier to water loss. Understanding these mechanisms will be critical to predicting the response of birds to climate change (Williams et al., 2012), especially in desert environments where birds may already be water limited.

MATERIALS AND METHODS

Capture of birds

We captured house sparrows with mist nets during August 2012 (N=11: summer birds) and January 2013 (N=8: winter birds) in Columbus, OH, USA (40°00′N, 83°10′W). In the 3 weeks prior to capture of the sparrows, the mean air temperature and dew point were 23 and 16°C, respectively, for the summer birds and −1 and −5°C for the winter birds. All birds were measured within 1–3 days of capture to minimize acclimation to laboratory conditions (temperature and dew point approximately 22 and 12°C, respectively). Sparrows were fed seeds and water *ad libitum*. Experiments were approved by IACUC at The Ohio State University (2009A0074-R1).

CWL

We measured CWL using standard flow-through respirometry (Tieleman and Williams, 2002; Ro and Williams, 2010). Our system separated CWL from respiratory water loss by placing a mask over the bird's bill to capture respiratory water. Before each measurement, we fasted the bird for 2–3 h to ensure post-absorptive conditions, then placed the bird in a water-jacketed stainless steel metabolic chamber (29.5×21.5×28 cm) with a sealed Plexiglas lid. A layer of mineral oil in the bottom of the chamber trapped feces to exclude them as a source of water in measurements. A circulating waterbath (Neslab RTE 7) maintained the chamber temperature at 30°C, a temperature within the thermoneutral zone for house sparrows (Hudson and Kimzey, 1966). To correct for differences in body mass between individuals, we used Meeh's equation (Meeh, 1879) with Rubner's constant of 10 (Rubner, 1883) to calculate the surface area (in cm^2) of each individual as:

$$\text{Surface area} = 10 \times \text{body mass}^{0.667}, \quad (1)$$

where body mass is in grams. This surface area calculation allowed us to express CWL as a function of skin surface area (Ro and Williams, 2010).

Attenuated ATR–FTIR

Fourier transform infrared spectroscopy (FTIR) passes infrared light (4000–400 cm^{-1}) through a sample to study the characteristic vibrations and associated vibrational structure of molecules. Chemical bonds within molecules vibrate at unique frequencies, and absorb infrared light at that same frequency. These characteristic absorptions are detected by FTIR as transmittance ratios and converted to absorbance peaks. The intensity of these peaks can provide information on the relative abundance of certain molecules or bond types, and the frequency at which these peaks are recorded provides information on relative bond strength, local environment and molecular ordering.

Attenuated total reflectance FTIR (ATR-FTIR) uses the optical properties of a crystal to measure chemical bond vibrations at the surface of a sample. Briefly, the sample is placed in direct contact with a crystal, and an infrared beam is passed into the crystal at or beyond the critical angle. The geometry of the crystal permits almost total internal reflection, thus only an evanescent light wave penetrates into the sample, then exits back through the crystal and to the infrared-sensitive detector. The depth of penetration (d) for this evanescent wave is calculated as:

$$d = \frac{\lambda}{2\pi\left(n_1^2 \sin^2\theta - n_1^2\right)^{1/2}}, \quad (2)$$

where λ is the wavelength of the infrared light, θ is the angle at which the light is passed through the crystal, and n_1 and n_2 are the refractive indices of the crystal and sample, respectively. In this study, λ ranged between 5.56 and 2.5 µm (1800 to 4000 cm^{-1}) and θ was 45 deg. The refractive indices of a ZnSe crystal and the SC are approximately 2.435 (Li, 1984) and 1.55 (Duck, 1990), respectively. Therefore, penetration depth of the evanescent wave was 0.531 µm at 1800 cm^{-1} and 1.115 µm at 4000 cm^{-1}, with intermediate values in between (Fig. 10). We analyzed the intensity and position of each peak in accordance with the maximum penetration depth calculated for that peak's wavelength.

We killed birds by cervical dislocation, then immediately cut and plucked the feathers surrounding the ventral apteria before sequentially pressing the left and right sides of the ventral apteria to a ZnSe crystal, and collected spectra with a Perkin Elmer (Spectrum 100) IR spectrometer equipped with an ATR accessory (Smart SpeculATR, Thermo Electron Corporation, Waltham, MA, USA) and a DTGS detector. We collected spectra at a resolution of 0.5 cm^{-1} based on an average of 10 scans for each side. To access deeper layers of the SC, we pressed Scotchbrand 600 transparent tape (3M, St Paul, MN, USA) to each side of the ventral apteria and removed each strip before collecting additional scans. We repeated this process 10 times to acquire spectra for 10 layers of each bird's SC. Tape strips were placed on a Teflon sheet and stored at −20°C until subsequent lipid analysis.

Spectral analysis

We used the peak analyzer function of OriginPro 8.6 (OriginLab Corporation, Northampton, MA, USA) software to identify the frequencies and areas of absorbance peaks between 4000 and 1800 cm^{-1}. For each spectrum, we subtracted the baseline and specified six peaks to be fitted: OH stretching peaks at ∼3500 and ∼3300 cm^{-1}, a CH stretching peak at ∼3080 cm^{-1}, a CH_2 asymmetric stretching peak at ∼2950 cm^{-1}, a CH_2 symmetric stretching peak at ∼2850 cm^{-1} and an H_2O combination band at ∼2100 cm^{-1}. We fitted Gaussian peaks to both OH stretching peaks and the H_2O combination band, and fitted Lorentzian peaks to the CH and CH_2 peaks. All peaks were fitted to an R^2 value of 0.98 or greater. For our analysis, we focused on the following three variables. (1) The frequency and relative areas of the OH stretching peaks at ∼3500 and ∼3300 cm^{-1}. These peaks provide information on the strength of intermolecular hydrogen bonding, and therefore can indicate the strength of bonds between lipid headgroups as well as the relative amount of water influenced by elements such as the sugar moiety of cerebrosides in the SC. The peak at ∼3500 cm^{-1} generally indicates hydrogen bond strength typical of free water or water perturbed by the presence of ions and solutes (Liu et al., 2004), whereas the peak at ∼3300 cm^{-1} indicates water in a more strongly hydrogen bonded environment with adjacent water molecules, sometimes in a tetrahedral bonding structure similar to that seen in ice (Du et al., 1993). As these peaks change in size, the relative positions of the peaks may change, and these peak positions may also provide information on the strength of hydrogen bonding, as low frequency peaks indicate stronger hydrogen bonding than high frequency peaks (Gallina et al., 2006). We assumed that the OH stretching contribution from lipid headgroups and sugar moieties was constant. (2) The frequency of the CH_2 symmetric stretching peak at ∼2800 cm^{-1} is an indicator of the relative amount of gauche defects within lipid alkyl chains. More gauche defects cause this peak to shift to a higher

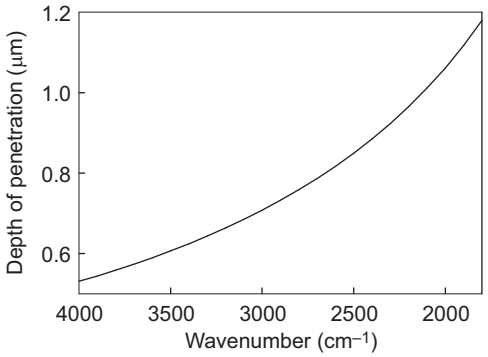

Fig. 10. Depth of penetration of an evanescent wave as a function of wavenumber. Calculations are based on the refractive indices of a ZnSe crystal and skin, and on an angle of incidence of 45 deg.

frequency. (3) The H_2O combination band is an indicator of SC water and increases in area as water content increases (Potts et al., 1985).

Lipid extraction

For each layer removed by tape stripping, we combined strips taken from the left and right sides of each bird to ensure each layer contained enough tissue for suitable lipid analysis, and submerged them in 10 ml ethyl acetate: methanol 1:4 (v:v) for 1 h to extract lipids. This procedure has been shown to extract lipids without extracting any tape-associated compounds (Weerheim and Ponec, 2001). After 1 h, the tape strips were removed from the test tube, placed on a Teflon sheet, and frozen for later protein analysis. We evaporated the solvent from the test tube at 50°C in a nitrogen manifold (N-EVAP, model 11155-O, Organomation Associates, Berlin, MA, USA), and re-dissolved the lipids in 800 µl of chloroform:methanol 2:1 (v:v). We then removed non-lipid material by adding 200 µl of distilled water, shaking the mixture, allowing it to settle into an aqueous and an organic phase, and extracting the organic phase for lipid analysis (Folch et al., 1957). The organic phase was evaporated and dissolved in 25 µl of chloroform:methanol 2:1 with 5 mg ml^{-1} butylated hydroxytoluene. The aqueous phase was evaporated and stored at −20°C for later analysis of protein content.

Quantification of intercellular lipids

We used 20×20 cm glass plates coated with silicic acid to a thickness of 0.25 mm (Adsorbosil-Plus 1, Altech, Deerfield, IL, USA) for thin layer chromatography to analyze the amount of lipid classes in the each layer of the SC. A 2:1 $CHCl_3$:MeOH solution run to the top of the plates removed contaminants prior to sample loading. Following this washing, we activated the plates by heating them in an oven for 30 min at 110°C, and then scored the silicic acid to create 13 separate lanes on each plate. For each sample, we ran one plate to detect relatively polar lipids, such as cerebrosides, ceramides and cholesterol, and a separate plate to detect non-polar lipids, such as free fatty acids, triacylglycerols, methyl esters and cholesterol esters. Because there was some variation in the degree of separation between ceramide classes on the polar plates, we classified ceramides based on their R_f values relative to the standard as either class I, the least polar, or class II, the most polar, because the polarity of ceramides has been shown to be important in CWL (Muñoz-Garcia et al., 2008a,b). We used a Hamilton syringe with a Teflon-coated tip to load a set of five standards composed of each lipid class dissolved in 2:1 chloroform:methanol at known concentrations on each plate. Our standard mixes were diluted 1/2, 1/4, 1/8 and 1/16, respectively, relative to the most concentrated standard to produce a range of lipid concentrations with which we compared the samples. After loading the standards, we loaded each sample into a lane, and then developed the plates. To separate polar lipids, we developed the plate with chloroform:methanol:water 40:10:1, run 10 cm from the bottom, followed by chloroform:methanol:acetic acid 190:9:1, run 15 cm from the bottom, and finally hexane:ethyl ether:acetic acid 70:30:1, run to the top. We developed non-polar plates with hexane: ethyl ether:acetic acid 80:20:2, run to the top (Ro and Williams, 2010). After developing the plates, we allowed them to dry, sprayed them with a solution of 3% cupric acetate in 8% phosphoric acid, and heated them in an oven for 30 min at 180°C to char lipids for quantification. We scanned the charred plates on a Hewlett-Packard scanner and quantified each lipid class with image analysis software (TN Image; Nelson, 2003).

To calculate the amount of SC removed by tape stripping and to standardize the lipid amount in each layer as a function of protein content, we quantified the amount of protein on each pair of tape strips. We combined each pair of strips with their associated aqueous extracts and immersed them in 4 ml of 1 mol l^{-1} NaOH for 2 h with shaking to solubilize the protein. After neutralizing the solution with 4 ml of 1 mol l^{-1} HCl and vortexing for 10 s, we used a Bio-Rad DC protein assay (Bio-Rad Laboratories, Hercules, CA, USA) and a FLUOstar Omega spectrophotometer (BMG Labtech, Cary, NC, USA) to calculate the optical density of each solution. We calculated the amount of protein (µg SC ml^{-1}) as:

$$\text{Protein} = (\text{OD}_{750} - 0.0212) \times (0.0019)^{-1}, \quad (3)$$

where OD_{750} is the optical density of the sample at 750 nm (Dreher et al., 1998). We then measured the surface area of each tape strip pair with Image J (NIH) and calculated the thickness of SC removed based on the finding that 100 µg cm^{-2} of protein corresponds to 1.9±0.2 µm of SC (Boncheva et al., 2009). We recognize that because our calculation of depth in the avian SC was based on an equation derived from human SC, our estimates of SC depth may not be exact. However, we observed the same trends in lipid content and FTIR-ATR absorbance whether we analyzed them as a function of strip number or as a function of depth in SC that we calculated, and therefore the trends we have found are robust. Furthermore, the main seasonal differences in the SC are differences in lipid content and corneodesmosome strength rather than corneocyte content, so we assume no differences in protein content between seasons (Rawlings et al., 1994).

Statistics

We performed statistical tests with SPSS 22.0 (IBM, Armonk, NY, USA), with statistical significance set at $P \leq 0.05$. To compare CWL between summer and winter house sparrows, we used a *t*-test. We used linear mixed models to compare protein content as a function of tape strip number, season and the interaction. We used linear mixed models to compare ATR-FTIR peak positions, peak areas and lipid content, respectively, as a function of depth, season and the interaction. Where interactions were insignificant, we dropped the interaction term and ran the linear mixed model to test only for main effects. We obtained estimates of significant interaction terms by running separate linear regression models for each season. To account for repeated measurements on individuals, we included individuals as a random variable in all linear mixed models. We used the curve estimation function in SPSS to determine whether each variable varied as a linear, logarithmic or inverse function with depth, and transformed variables as necessary. Values are presented as means±s.e.

Acknowledgements

We thank members of the Allen and Williams labs and Dave Denlinger for their valuable feedback throughout this study. We also thank Ellen Adams for her assistance with ATR-FTIR. Finally, we thank the managers at OSU Waterman Farm and Paul Hurtado for their assistance in obtaining house sparrows.

Competing interests

The authors declare no competing or financial interests.

Author contributions

A.M.C. contributed to the development of concepts for this research, performed experiments and data analysis, and prepared the manuscript. H.C.A. contributed to the development of concepts related to ATR-FTIR and revised the manuscript. J.B.W. contributed to the development of concepts related to whole-organism physiology and thin layer chromatography, and revised the manuscript.

Funding

This research was supported by National Science Foundation grant NSF-CHE 1111762 to H.C.A. and grant 2008469 of the US-Israel Binational National Science Foundation to J.B.W.

Supplementary material

Supplementary material available online at
http://jeb.biologists.org/lookup/suppl/doi:10.1242/jeb.125310/-/DC1

References

Adams, E. M. and Allen, H. C. (2013). Palmitic acid on salt subphases and in mixed monolayers of cerebrosides: application to atmospheric aerosol chemistry. *Atmosphere* **4**, 315-336.

Alonso, A., Meirelles, N. C., Yushmanov, V. E. and Tabak, M. (1996). Water increases the fluidity of intercellular membranes of stratum corneum: correlation with water permeability, elastic, and electrical resistance properties. *J. Invest. Dermatol.* **106**, 1058-1063.

Bach, D., Sela, B. and Miller, I. R. (1982). Compositional aspects of lipid hydration. *Chem. Phys. Lipids* **31**, 381-394.

Bartholomew, G. A. (1972). The water economy of seed-eating birds that survive without drinking. *Proc. Int. Ornithol. Congr.* **15**, 1-16.

Bommannan, D., Potts, R. O. and Guy, R. H. (1990). Examination of stratum corneum barrier function in vivo by infrared spectroscopy. *J. Invest. Dermatol.* **95**, 403-408.

Boncheva, M., de Sterke, J., Caspers, P. J. and Puppels, G. J. (2009). Depth profiling of Stratum corneum hydration in vivo: a comparison between

conductance and confocal Raman spectroscopic measurements. *Exp. Dermatol.* **18**, 870-876.
Bonté, F., Saunois, A., Pinguet, P. and Meybeck, A. (1997). Existence of a lipid gradient in the upper stratum corneum and its possible biological significance. *Arch. Dermatol. Res.* **289**, 78-82.
Bouwstra, J. A. (1997). The skin barrier, a well-organized membrane. *Colloids Surf. A Physicochem. Eng. Aspects* **123-124**, 403-413.
Bouwstra, J. A., Dubbelaar, F. E. R., Gooris, G. S. and Ponec, M. (2000). The lipid organisation in the skin barrier. *Acta Derm. Venereol.* **80**, 23-30.
Casal, H. L. and McElhaney, R. N. (1990). Quantitative determination of hydrocarbon chain conformational order in bilayers of saturated phosphatidylcholines of various chain lengths by fourier transform infrared spectroscopy. *Biochemistry* **29**, 5423-5427.
Champagne, A. M., Munoz-Garcia, A., Shtayyeh, T., Tieleman, B. I., Hegemann, A., Clement, M. E. and Williams, J. B. (2012). Lipid composition of the stratum corneum and cutaneous water loss in birds along an aridity gradient. *J. Exp. Biol.* **215**, 4299-4307.
Chapman, S. J. and Walsh, A. (1990). Desmosomes, corneosomes and desquamation. An ultrastructural study of adult pig epidermis. *Arch. Dermatol. Res.* **282**, 304-310.
Chapman, S. J., Walsh, A., Jackson, S. M. and Friedmann, P. S. (1991). Lipids, proteins and corneocyte adhesion. *Arch. Dermatol. Res.* **283**, 167-173.
Clement, M. E., Munoz-Garcia, A. and Williams, J. B. (2012). Cutaneous water loss and covalently bound lipids of the stratum corneum in nestling house sparrows (*Passer domesticus* L.) from desert and mesic habitats. *J. Exp. Biol.* **215**, 1170-1177.
Comesaña, J. F., Otero, J. J., García, E. and Correa, A. (2003). Densities and viscosities of ternary systems of water plus glucose plus sodium chloride at several temperatures. *J. Chem. Eng. Data* **48**, 362-366.
Cox, R. M., Muñoz-Garcia, A., Jurkowitz, M. S. and Williams, J. B. (2008). Beta-glucocerebrosidase activity in the stratum corneum of house sparrows following acclimation to high and low humidity. *Physiol. Biochem. Zool.* **81**, 97-105.
Dawson, W. R. (1982). Evaporative losses of water by birds. *Comp. Biochem. Physiol. A Physiol.* **71**, 495-509.
Dreher, F., Arens, A., Hostynek, J. J., Mudumba, S., Ademola, J. and Maibach, H. I. (1998). Colorimetric method for quantifying human Stratum corneum removed by adhesive-tape-stripping. *Acta Derm. Venereol.* **78**, 186-189.
Du, Q., Superfine, R., Freysz, E. and Shen, Y. R. (1993). Vibrational spectroscopy of water at the vapor/water interface. *Phys. Rev. Lett.* **70**, 2313-2316.
Duck, F. A. (1990). *Physical Properties of Tissues: A Comprehensive Reference Book*, pp. 62-63. San Diego, CA: Academic Press Ltd.
Folch, J., Lees, M. and Stanley, G. H. S. (1957). A simple method for the isolation and purification of total lipids from animal tissues. *J. Biol. Chem.* **226**, 497-509.
Freinkel, R. K. and Aso, K. (1969). Esterification of cholesterol in skin. *J. Invest. Dermatol.* **52**, 148-154.
Freinkel, R. K. and Aso, K. (1971). Esterification of cholesterol by epidermis. *Biochim. Biophys. Acta* **239**, 98-102.
Fuchs, K. and Kaatze, U. (2001). Molecular dynamics of carbohydrate aqueous solutions. Dielectric relaxation as a function of glucose and fructose concentration. *J. Phys. Chem. B* **105**, 2036-2042.
Gallina, M. E., Sassi, P., Paolantoni, M., Morresi, A. and Cataliotti, R. S. (2006). Vibrational analysis of molecular interactions in aqueous glucose solutions. Temperature and concentration effects. *J. Phys. Chem. B* **110**, 8856-8864.
Golden, G. M., Guzek, D. B., Harris, R. R., McKie, J. E. and Potts, R. O. (1986). Lipid thermotropic transitions in human stratum corneum. *J. Invest. Dermatol.* **86**, 255-259.
Gu, Y., Munoz-Garcia, A., Brown, J. C., Ro, J. and Williams, J. B. (2008). Cutaneous water loss and sphingolipids covalently bound to corneocytes in the stratum corneum of house sparrows Passer domesticus. *J. Exp. Biol.* **211**, 1690-1695.
Haugen, M., Williams, J. B., Wertz, P. and Tieleman, B. I. (2003). Lipids of the stratum corneum vary with cutaneous water loss among larks along a temperature-moisture gradient. *Physiol. Biochem. Zool.* **76**, 907-917.
Holleran, W. M., Ginns, E. I., Menon, G. K., Grundmann, J. U., Fartasch, M., McKinney, C. E., Elias, P. M. and Sidransky, E. (1994). Consequences of beta-glucocerebrosidase deficiency in epidermis. ultrastructure and permeability barrier alterations in gaucher disease. *J. Clin. Invest.* **93**, 1756-1764.
Hudson, J. W. and Kimzey, S. L. (1966). Temperature regulation and metabolic rhythms in populations of the house sparrow, Passer domesticus. *Comp. Biochem. Physiol.* **17**, 203-217.
Lewis, R. N. A. H. and McElhaney, R. N. (2007). Fourier transform infrared spectroscopy in the study of lipid phase transitions in model and biological membranes: practical consierations. In *Methods in Molecular Biology*, Vol 400, *Methods in Membrane Lipids* (ed. A. M. Dopico), pp. 207-226. Totowa, NJ: Humana Press Inc.
Li, H. H. (1984). Refractive index of ZnS, ZnSe, and ZnTe and its wavelength and temperature derivatives. *J. Phys. Chem. Ref. Data* **13**, 103-150.
Liang, G. L., Noid, D. W., Sumpter, B. G. and Wunderlich, B. (1994). Gauche defects, positional disorder, dislocations, and slip planes in crystals of long methylene sequences. *J. Phys. Chem.* **98**, 11739-11744.
Liu, D., Ma, G., Levering, L. M. and Allen, H. C. (2004). Vibrational spectroscopy of aqueous sodium halide solutions and air-liquid interfaces: observation of increased interfacial depth. *J. Phys. Chem. B* **108**, 2252-2260.
Maggio, B., Fanani, M. L., Rosetti, C. M. and Wilke, N. (2006). Biophysics of sphingolipids II. Glycosphingolipids: an assortment of multiple structural information transducers at the membrane surface. *Biochim. Biophys. Acta Biomembr.* **1758**, 1922-1944.
Matoltsy, A. G. (1969). Keratinization of the avian epidermis: an ultrastructural study of the newborn chick skin. *J. Ultrastruct. Res.* **29**, 438-458.
Meeh, K. (1879). Oberflächenmessungen des menschlichen Körpers. *Z. Biol.* **15**, 426-458.
Menon, G. K., Brown, B. E. and Elias, P. M. (1986). Avian epidermal differentiation: role of lipids in permeability barrier formation. *Tissue Cell* **18**, 71-82.
Meuwissen, M. E. M. J., Janssen, J., Cullander, C., Junginger, H. E. and Bouwstra, J. A. (1998). A cross-section device to improve visualization of fluorescent probe penetration into the skin by confocal laser scanning microscopy. *Pharm. Res.* **15**, 352-356.
Miranda, P. B., Du, Q. and Shen, Y. R. (1998). Interaction of water with a fatty acid Langmuir film. *Chem. Phys. Lett.* **286**, 1-8.
Muñoz-Garcia, A. and Williams, J. B. (2007). Cutaneous water loss and lipids of the stratum corneum in dusky antbirds, a lowland tropical bird. *Condor* **109**, 59-66.
Muñoz-Garcia, A., Ro, J., Brown, J. C. and Williams, J. B. (2006). Identification of complex mixtures of sphingolipids in the stratum corneum by reversed-phase high-performance liquid chromatography and atmospheric pressure photospray ionization mass spectrometry. *J. Chromatogr. A* **1133**, 58-68.
Muñoz-Garcia, A., Cox, R. M. and Williams, J. B. (2008a). Phenotypic flexibility in cutaneous water loss and lipids of the stratum corneum in house sparrows (Passer domesticus) following acclimation to high and low humidity. *Physiol. Biochem. Zool.* **81**, 87-96.
Muñoz-Garcia, A., Ro, J., Brown, J. C. and Williams, J. B. (2008b). Cutaneous water loss and sphingolipids in the stratum corneum of house sparrows, Passer domesticus L., from desert and mesic environments as determined by reversed phase high-performance liquid chromatography coupled with atmospheric pressure photospray ionization mass spectrometry. *J. Exp. Biol.* **211**, 447-458.
Nelson, T. J. (2003). IMAL. Available at http://www.randombio.com/imal.html.
Ohman, H. and Vahlquist, A. (1994). In vivo studies concerning a pH gradient in human stratum corneum and upper epidermis. *Acta Derm. Venereol.* **74**, 375-379.
Paolantoni, M., Sassi, P., Morresi, A. and Santini, S. (2007). Hydrogen bond dynamics and water structure in glucose-water solutions by depolarized Rayleigh scattering and low-frequency Raman spectroscopy. *J. Chem. Phys.* **127**, 024504.
Potts, R. O. and Francoeur, M. L. (1990). Lipid biophysics of water loss through the skin. *Proc. Natl. Acad. Sci. USA* **87**, 3871-3873.
Potts, R. O., Guzek, D. B., Harris, R. R. and McKie, J. E. (1985). A noninvasive, in vivo technique to quantitatively measure water concentration of the stratum corneum using attenuated total-reflectance infrared spectroscopy. *Arch. Dermatol. Res.* **277**, 489-495.
Puhvel, S. M. (1975). Esterification of 4-^{14}C Cholesterol by cutaneous bacteria (Staphylococcus epidermidis, *Propionibacterium acnes*, and *Propionibacterium granulosum*). *J. Invest. Dermatol.* **64**, 397-400.
Rawlings, A. V., Hope, J., Rogers, J., Mayo, A. M., Hope, J. and Scott, I. R. (1994). Abnormalities in stratum corneum structure, lipid composition and desmosomal degradation in soap induced winter xerosis. *J. Soc. Cosmet. Chem.* **45**, 203-220.
Rawlings, A. V., Watkinson, A., Harding, C. R., Ackerman, C., Banks, J., Hope, J. and Scott, I. R. (1995). Changes in stratum corneum lipid and desmosome structure together with water barrier function during mechanical stress. *J. Soc. Cosmet. Chem.* **46**, 141-151.
Ro, J. and Williams, J. B. (2010). Respiratory and cutaneous water loss of temperate-zone passerine birds. *Comp. Biochem. Physiol. A Mol. Integr. Physiol.* **156**, 237-246.
Rubner, M. (1883). Über den Ein fluss der Körpergrösse auf Stoff- und Kraftwechsel. *Zeit. Biol.* **19**, 535-562.
Simon, M., Bernard, D., Minondo, A.-M., Camus, C., Fiat, F., Corcuff, P., Schmidt, R. and Serre, G. (2001). Persistence of both peripheral and non-peripheral corneodesmosomes in the upper stratum corneum of winter xerosis skin versus only peripheral in normal skin. *J. Invest. Dermatol.* **116**, 23-30.
Simonetti, O., Kempenaar, J. A., Ponec, M., Hoogstraate, A. J., Bialik, W., Schrijvers, A. H. G. J. and Boddé, H. E. (1995). Visualization of diffusion pathways across the stratum corneum of native and in-vitro-reconstructed epidermis by confocal laser scanning microscopy. *Arch. Dermatol. Res.* **287**, 465-473.
Tang, C. Y., Huang, Z. and Allen, H. C. (2011). Interfacial water structure and effects of Mg^{2+} and Ca^{2+} binding to the COOH Headgroup of a Palmitic acid monolayer studied by sum frequency spectroscopy. *J. Phys. Chem. B* **115**, 34-40.
Tieleman, B. I. and Williams, J. B. (2002). Cutaneous and respiratory water loss in larks from arid and mesic environments. *Physiol. Biochem. Zool.* **75**, 590-599.

Journal of Experimental Biology

Warner, R. R., Myers, M. C. and Taylor, D. A. (1988). Electron probe analysis of human skin: determination of the water concentration profile. *J. Invest. Dermatol.* **90**, 218-224.
Weerheim, A. and Ponec, M. (2001). Determination of stratum corneum lipid profile by tape stripping in combination with high-performance thin-layer chromatography. *Arch. Dermatol. Res.* **293**, 191-199.
Wertz, P. W. and Downing, D. T. (1982). Glycolipids in mammalian epidermis: structure and function in the water barrier. *Science* **217**, 1261-1262.
Wertz, P. W. and Downing, D. T. (1987). Covalently bound omega-hydroxyacylsphingosine in the stratum corneum. *Biochim. Biophys. Acta* **917**, 108-111.
Williams, J. B. and Tieleman, B. I. (2000). Flexibility in basal metabolic rate and evaporative water loss among hoopoe larks exposed to different environmental temperatures. *J. Exp. Biol.* **203**, 3153-3159.
Williams, J. B. and Tieleman, B. I. (2005). Physiological adaptation in desert birds. *Bioscience* **55**, 416-425.
Williams, J. B., Muñoz-Garcia, A. and Champagne, A. (2012). Climate change and cutaneous water loss of birds. *J. Exp. Biol.* **215**, 1053-1060.
Wolkers, W. F., Oliver, A. E., Tablin, F. and Crowe, J. H. (2004). A Fourier-transform infrared spectroscopy study of sugar glasses. *Carbohydr. Res.* **339**, 1077-1085.